XIII ICSMFE, 1994, New Delhi, India / XIII CIMSTF, 1994, New Delhi, Inde

LIQUEFACTION DURING THE 1886 CHARLESTON EARTHQUAKE

LA LIQUEFACTION PENDANT LE TREMBLEMENT DE TERRE DE CHARLESTON EN 1886

G.J. Rix[1] *J.S. Indridason*[2]

[1]Assistant Professor, [2]Graduate Research Assistant
Georgia Institute of Technology
Atlanta, Georgia, U.S.A.

SYNOPSIS: An earthquake near Charleston, South Carolina in 1886 caused significant liquefaction-related damage. A strain-based approach was used to evaluate the liquefaction potential of six Charleston-area sites to compare with the observed behavior. The basis of the approach is that the development of excess pore water pressure is directly related to the shear strain level induced by an earthquake. In situ seismic tests were used to measure the near-surface shear wave velocity profile. Using synthetic ground motions and one-dimensional site response analyses, the shear strain in the liquefiable layers was calculated. At sites with similar maximum accelerations, the shear strains differed substantially because of differences in shear wave velocity profiles. Pore pressure ratios were predicted using the calculated shear strains and the equivalent number of cycles in the synthetic motion. The predicted pore pressures at the six sites are consistent with the observed liquefaction behavior.

INTRODUCTION

On August 31, 1886 a large earthquake near Charleston, South Carolina caused substantial damage to much of the southeastern United States. The maximum epicentral intensity (Modified Mercalli scale) was X and damage associated with a Modified Mercalli intensity of VIII occurred over more than 40,000 km^2 (Bollinger, 1977). Seismological evidence suggests that the body wave magnitude (m_b) of the earthquake was between 6.6 and 6.9 and that the surface wave magnitude (M_s) was about 7.5 to 7.7 (Nuttli et al., 1989). Estimated maximum ground surface accelerations were between 0.5 and 0.6 g, although Chapman et al. (1989) have proposed that they could have been as large as 1.0 g.

Liquefaction-related ground failures were responsible for much of the damage caused by the earthquake. Dutton (1889) reported numerous first-hand observations of sand boils and craters following the earthquake and recent paleo-liquefaction investigations (Obermeier et al., 1987) have revealed other locations where liquefaction occurred.

Martin and Clough (1990) studied the liquefaction caused by the 1886 earthquake from the point of view of geotechnical earthquake engineering. Cone penetration tests (CPT) and standard penetration tests (SPT) were performed at 16 sites in the Charleston area to evaluate the liquefaction susceptibility of near-surface soils. An important conclusion of their research is that if the surface wave magnitude of the 1886 earthquake was about 7.5 as suggested by seismological evidence, maximum acceleration levels of about 0.3 to 0.4 g are sufficient to explain the observed liquefaction features. These acceleration levels are less than the 0.5 to 0.6 g levels suggested by seismological studies. Martin and Clough concluded that the magnitude of the earthquake based on their geotechnical study of the Charleston-area soils was likely between 6.0 and 7.5.

The objective of this study was to use a strain-based approach to evaluate the liquefaction potential of six sites in the Charleston area. In situ seismic tests were performed at the sites to measure the shear wave velocity profile. These profiles along with synthetic ground motions representative of the 1886 earthquake were used to calculate the shear strain in the liquefiable layers. Pore pressure ratios at the six sites were predicted using a model that expresses the pore pressure ratio as a function of the cyclic shear strain and the number of cycles of loading. Finally, the predicted pore pressure ratios were compared to the extent of the liquefaction that occurred in the 1886 earthquake.

STRAIN-BASED APPROACH

Liquefaction is caused by the development of excess pore pressure during earthquake shaking. The most commonly used method of evaluating liquefaction susceptibility is a stress-based, empirical approach employing SPT blow count (Seed et al., 1983). However, the development of excess pore pressure in soils is more closely related to the level of strain induced by the earthquake than the stress level (Dobry et al., 1982). Therefore, an approach based on cyclic strains should provide a better method of evaluating liquefaction susceptibility.

The threshold strain, γ_t, is the shear strain needed to initiate development of excess pore pressure. In many cohesionless soils, this threshold value is about 0.01 percent as shown in Fig. 1. Laboratory tests on a variety of cohesionless soils demonstrate that the development of pore pressures depends on the level of cyclic strain, number of cycles of loading and overconsolidation ratio but is independent of relative density, grain size distribution, and sample preparation methods (Vucetic and Dobry, 1988; Ladd et al., 1989).

The cyclic shear strain induced by an earthquake can be calculated:

$$\gamma = \frac{a_{max}\ \sigma_0\ r_d}{(G/G_{max})_\gamma\ G_{max}} \qquad (1)$$

where γ is the strain, a_{max} is the maximum ground surface acceleration in g's, G_{max} is the initial tangent shear modulus, $(G/G_{max})_\gamma$ is the shear modulus reduction factor at a strain equal to γ, σ_0 is the total overburden stress, and r_d is a reduction factor to account for the deformability of the soil (Seed and Idriss, 1971). Values of the initial tangent shear modulus are obtained from in situ seismic methods.

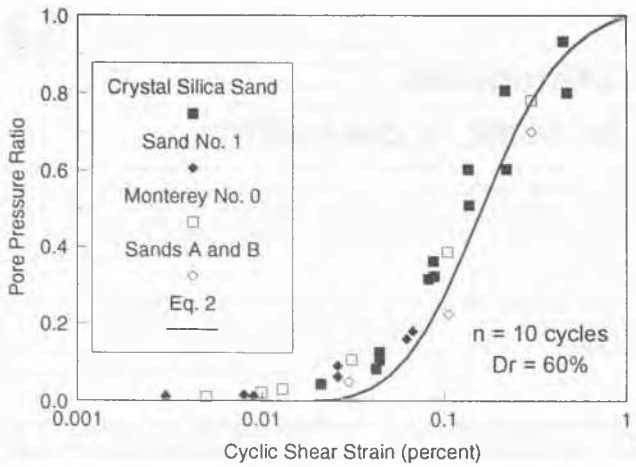

Fig. 1 Pore pressure ratio vs. shear strain (after Ladd et al., 1989)

The simplest calculation is to compare the cyclic shear strain in a liquefiable layer to the threshold strain. If γ/γ_t is less than one, excess pore pressures will not develop during earthquake shaking. The use of the threshold strain provides a conservative estimate of liquefaction susceptibility because the threshold strain is the strain necessary to initiate development of excess pore pressure. Liquefaction will likely not occur until the excess pore pressure increases.

The cyclic strain approach can be extended to predict the actual buildup of pore pressures using relationships between pore pressure ratio and cyclic strain like that shown in Fig. 1. Cyclic strains induced by an earthquake can be calculated using simple expressions like Eq. 1 or more rigorous means such as SHAKE (Schnabel et al., 1972). Vucetic and Dobry (1988) give an expression for calculating the pore pressure ratio based on the shear strain and number of cycles of loading:

$$u^* = \frac{2.70\, n\, (\gamma - 0.02)^{1.7}}{1 + 2.6\, n\, (\gamma - 0.02)^{1.7}} \qquad (\gamma \geq 0.02\%) \qquad (2)$$

where u^* is the pore pressure ratio and n is the number of cycles. This relationship between u^* and γ is plotted in Fig. 1.

The cyclic strain approach has been successfully used to predict liquefaction caused by the 1979 Imperial Valley earthquake and the 1981 Westmorland earthquake by Bierschwale (1984) and the 1983 Borah Peak earthquake by Stokoe et al. (1989).

SITE DESCRIPTIONS

The area surrounding Charleston, South Carolina consists of low-lying swamps and marshlands with higher-elevation ridges composed of marine and fluvial sediments that run parallel to the coastline. Much of the observed liquefaction occurred in soil deposits that flank these ridges. The general soil profile usually consists of sand of various densities (marine/fluvial deposits) at shallow depths with clay layers (lagoonal deposits) interbedded in deeper deposits. The Cooper-Marl formation, a very stiff silty clay, is usually encountered at depths ranging from 9 to 20 m. The groundwater table is usually within one or two meters of the surface (Martin and Clough, 1990).

The study by Martin and Clough (1990) was used as a guide to select sites with a wide range of liquefaction behavior during the 1886 earthquake. The sites selected were Mt. Pleasant Pits, Oakland Plantation, Sod Farm, Hollywood Canal, Ten Mile Hill and Montague Avenue. Liquefaction features at these sites caused by the 1886 earthquake ranged from none (Mt. Pleasant Pits) to extensive (Ten Mile Hill).

The grain size distribution curve for a sample of liquefiable sand from an exposed borrow pit at the Oakland Plantation site is shown as a solid line in Fig. 2. The sand is an SP. Also shown by the shaded area in Fig. 2 is the range of grain size distribution curves for the four different sands represented in Fig. 1. It is evident that cohesionless soils with a broad range of grain size distributions all have a unique curve of u^* vs. γ (Fig. 1). Because the sand from the Charleston-area site falls within this range, Eq. 2 is considered to define the relationship between u^* and γ for the sands in this study.

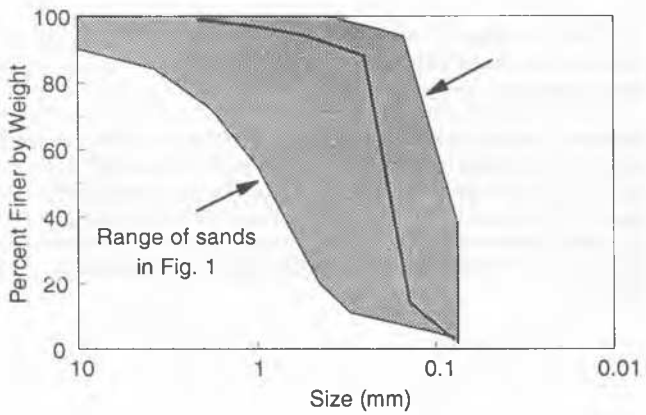

Fig. 2 Grain size curve of sand from Oakland Plantation site

At each of the six sites, a Spectral Analysis of Surface Waves (SASW) test was performed to measure the shear wave velocity profile. The SASW test procedure is described by Stokoe et al. (1988). Surface wave tests were performed as close as possible to the penetration tests and borings by Martin and Clough (1990). Plots of shear wave velocity vs. depth for the six sites are shown in Fig. 3. Hollywood Canal, Sod Farm, and Oakland Plantation have similar profiles that contain a low velocity layer (V_s = 100 to 150 m/s) between depths of 2 and 4 m. Also, the shear wave velocity at greater depths remains less than 400 m/s for these sites. Ten Mile Hill, Montague Avenue, and Mt. Pleasant Pits have shear wave velocities that increase with depth. The shear wave velocities at the Montague Avenue site are clearly greater than at the other sites.

LIQUEFACTION POTENTIAL ANALYSES

Evaluations of the liquefaction potential for the six sites were performed using SHAKE (Schnabel et al., 1972). SHAKE performs a total stress analysis that models the response of a horizontally layered site to a vertically propagating shear wave from an underlying formation. Each layer is characterized by a thickness, unit weight, shear modulus and damping ratio. An equivalent linear approach is used to incorporate nonlinear soil behavior. Initial tangent shear moduli (G_{max}) were obtained from the surface wave tests. Modulus reduction (G/G_{max} vs. γ) and damping ratio (D vs. γ) curves developed for sands by Seed et al. (1986) and for clays by Dobry and Vucetic (1991) were used to describe the variation of shear modulus and damping ratio with shear strain. The modulus reduction and damping ratio curves reported by Seed et al. and Dobry and Vucetic are considered to be representative of a broad range of sands and clays, respectively, including those encountered in the Charleston area. Dobry and Vucetic give modulus reduction and damping ratio curves that are a function of the plasticity index (PI) of the soil. Curves for a PI equal to 50 were chosen based on the average plasticity index of clays in the Charleston area.

Another input for the SHAKE analyses is an acceleration-time history for the 1886 Charleston earthquake. Since no actual ground motion recordings exist for the 1886 earthquake, a synthetic acceleration-time history generated by Chapman et al. (1989) was used. The synthetic motion is shown in Fig. 4.

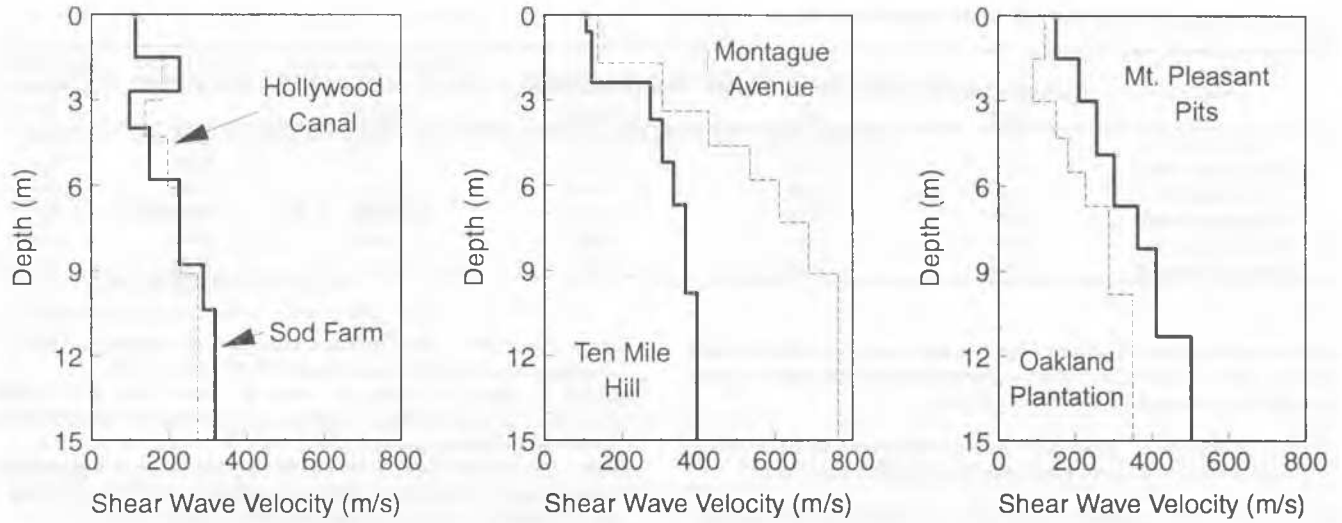

Fig. 3 Shear wave velocity profiles

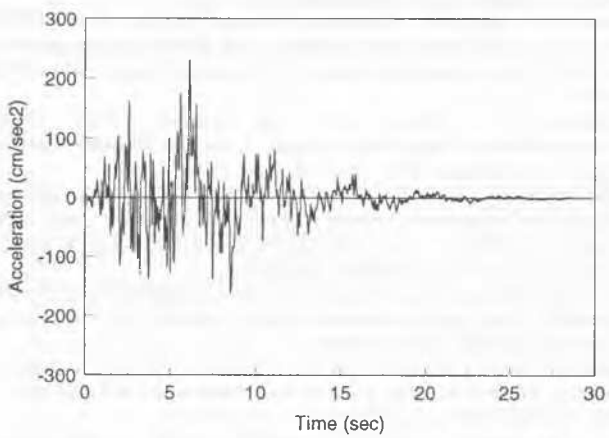

Fig. 4 Synthetic ground motion used for SHAKE analyses

The motion shown in Fig. 4 is assumed to be the motion at the top of the Cooper-Marl formation. SHAKE is used to propagate this motion upward through the near-surface layers at each of the six sites. Since the sites are at different distances from the epicenter, the motion in Fig. 4 must be scaled before being used in SHAKE. The attenuation relationship used in this study to determine the peak ground acceleration at each site is given by Nuttli et al. (1984):

$$a_{max} = 0.00379e^{1.15m_b}(R^2 + h_{min}^2)^{-0.415}e^{-0.00589R} \quad (3)$$

where a_{max} is the peak ground acceleration in g's, R is the epicentral distance in km, m_b is the body wave magnitude of the earthquake, and h_{min} is the minimum focal depth in km. The minimum focal depth is given by.

$$h_{min} = 0.0186e^{1.05m_b} \quad (4)$$

Eqs. 3 and 4 are valid for $m_b > 4.5$. Nuttli et al. (1989) have estimated the body wave magnitude of the 1886 earthquake to be about 6.7.

Once the earthquake motion was scaled, SHAKE was used to calculate the cyclic shear strain in the liquefiable layers. With these values of shear strain, the pore pressure ratio at each of the six sites was calculated using Eq. 2. The number of equivalent cycles for the ground motion in Fig. 4 is 5.7 (Seed et al., 1975). Thus, n was set equal to 5.7 in Eq. 2.

Table 1 summarizes the calculations performed to predict the pore pressure ratio at the six sites. Included in Table 1 are the values of shear strain in the liquefiable layer predicted by Eq. 1 for each of the six sites. At four of the six sites the effective shear strains from the SHAKE analysis are substantially larger than those from Eq. 1. At the remaining two sites (Montague Avenue and Mt. Pleasant Pits), the strains are approximately equal. The shear wave velocity profiles explain the differences. At the Hollywood Canal, Sod Farm, Ten Mile Hill, and Oakland Plantation sites, the shear strains are concentrated in the low velocity layers. At the Montague Avenue and Mt. Pleasant Pits sites, the shear wave velocities increase uniformly with depth. As a result, the shear strains are more uniform with depth and a simplified expression such as Eq. 1 more accurately predicts the shear strain level.

Differences in shear wave velocity profiles also explain the differences in the effective shear strain level for sites with similar maximum accelerations. The first four sites listed in Table 1 have maximum accelerations that lie in a narrow range from 0.56 to 0.62 g, yet the shear strains differ substantially. The Sod Farm and Hollywood Canal sites have low velocity layers between depths of 3 and 4 m where the shear strains are largest. Ten Mile Hill has a low velocity surface layer where the largest strain occurs. Furthermore, the shear wave velocities in the upper 15 m are less than 400 m/s at these three sites. The smallest acceleration occurs at Montague Avenue which is the stiffest of the four sites.

The last column of the table lists whether liquefaction features caused by the 1886 earthquake were observed at the site. The predicted pore pressure ratios are reasonably consistent with the observed behavior. Liquefaction features were observed at the Sod Farm and Hollywood Canal sites where the predicted pore pressure ratios are essentially 1.0. At the Ten Mile Hill site, liquefaction features were observed although the predicted pore pressure ratio is only 0.78. It is likely that the discrepancy results from the simplified one-dimensional, total stress analysis used in this study. In the authors' opinion, however, the predicted pore pressure ratio gives a sufficient indication of the liquefaction potential of the site. At the remaining three sites, lower values of predicted pore pressure ratio agree with the lack of liquefaction features at the sites.

CONCLUSIONS

A strain-based approach was used to predict the liquefaction behavior at six sites in the Charleston, South Carolina area during the 1886 earthquake. In

Table 1 Summary of Predicted and Observed Liquefaction Behavior

Site	Epicentral Distance (km)	Maximum Acceleration (g)	Shear Strain from Eq. 1 (percent)	Effective Shear Strain from SHAKE Analysis (percent)	Predicted Pore Pressure Ratio	Liquefaction Observed in 1886
Sod Farm	6.4	0.62	0.27	1.52	1.00	Yes
Hollywood Canal	8.0	0.59	0.13	1.18	0.99	Yes
Ten Mile Hill	8.0	0.59	0.10	0.41	0.78	Yes
Montague Avenue	9.6	0.56	0.02	0.01	0.00	No
Mt. Pleasant Pits	24.1	0.41	0.03	0.03	0.01	No
Oakland Plantation	31.0	0.34	0.07	0.18	0.41	No

all six cases the approach predicted pore pressure ratios that were consistent with the observed liquefaction behavior. There are several advantages of using a strain based approach for liquefaction analyses:

1) The development of excess pore water pressure during dynamic loading depends more on the cyclic shear strain than the cyclic stress level.

2) The cyclic strain approach predicts the actual development of excess pore pressure instead of only distinguishing between liquefaction and no liquefaction.

3) The cyclic strain approach is more theoretically sound than existing empirical methods.

The viability of using cyclic strains as a basis for predicting liquefaction behavior needs to be demonstrated at other sites to establish confidence in the approach.

An uncertainty in the analyses performed for this study is the synthetic acceleration-time history used to represent the 1886 Charleston earthquake. An apparent inconsistency is that the surface wave magnitude of the 1886 Charleston earthquake has been estimated to be about 7.5 to 7.7, yet the number of equivalent cycles in the synthetic motion (n = 5.7) is less than expected for a magnitude 7.5 earthquake (n = 15). The number of cycles in the synthetic motion is more consistent with a magnitude 6 earthquake (n = 5 to 6) (Seed et al., 1983).

ACKNOWLEDGMENTS

The authors are grateful to Mr. W.M. Camp, III for his assistance in coordinating the field work and to Dr. M.C. Chapman for making the synthetic ground motions available. This work was performed as part of National Science Foundation Grant No. BCS-9110173. The authors are grateful to the National Science Foundation and Dr. Clifford J. Astill for their support.

REFERENCES

Bierschwale, J.G. (1984). Analytical evaluation of liquefaction potential of sands subjected to the 1981 Westmorland earthquake. Geotechnical Engineering Report GR-84-15, Geotechnical Engineering Center, The University of Texas at Austin, 231 pp.

Bollinger, G.A. (1977). Reinterpretation of the intensity data for the 1886 Charleston, South Carolina earthquake. US Geological Survey Professional Report 1028, 17-32.

Chapman, M.C., Bollinger, M., Sibol, M.S. and Stephenson, D.E. (1989). The influence of coastal plain sedimentary wedge on strong ground motions from the 1886 Charleston, South Carolina earthquake. *Earthquake Spectra* 6(4), Earthquake Engineering Research Institute, 617-640.

Dobry, R., Ladd, R.S., Yokel, F.Y., Chung, R.M. and Powell, M.D., (1982). Prediction of pore water pressure buildup and liquefaction of sand during earthquakes by the cyclic strain method. National Bureau of Standards Building Science Series 138, Washington, D.C., 154 pp.

Dutton, C.E. (1889). The Charleston earthquake of August 31, 1886. US Geological Survey Ninth Annual Report 1887-1888, 203-528.

Ladd, R.S., Dobry, R., Dutko, P., Yokel, F.Y. and Chung, R.M. (1989). Pore-water pressure buildup in clean sands because of cyclic straining. *Geotechnical Testing Journal* 12(1), 77-86.

Martin, J.R.,II and Clough, G.W. (1990). Implications from a geotechnical investigation of liquefaction phenomena associated with seismic events in the Charleston, SC area. US Geological Survey Report, 414 pp.

Nuttli, O.W., Rodrigues, R. and Herrmann, R.B. (1984). Strong ground motion studies for South Carolina earthquakes. NUREG/CR-3755, U.S. Nuclear Regulatory Commission, Washington, D.C.

Nuttli, O.W., Jost, M.L., Herrmann, R.B. and Bollinger, G.A. (1989). Numerical models of the rupture mechanics and far-field ground motion of the 1886 South Carolina earthquake. US Geological Survey Bulletin No. 1586.

Obermeier, S.F., Weems, F.E. and Jacobson, R.B. (1987). Earthquake-induced liquefaction features in the coastal South Carolina region. US Geological Survey Open-File Report 87-504.

Schnabel, P.B., Lysmer, J. and Seed, H.B. (1972). SHAKE: a computer program for earthquake response analysis of horizontally layered sites. Report No. EERC 72-12, Earthquake Engineering Research Center, University of California, Berkeley, California.

Seed, H.B., Idriss, I.M. and Arango, I. (1983). Evaluation of liquefaction potential using field performance data," *Journal of Geotechnical Engineering* 109(3), ASCE, 458-482.

Seed, H.B., Wong, R.T., Idriss, I.M. and Tokimatsu, K. (1986). Moduli and damping factors for dynamic analyses of cohesionless soils. *Journal of Geotechnical Engineering* 112(11), ASCE, 1016-1032.

Seed, H.B. and Idriss, I.M. (1971). Simplified procedure for evaluating soil liquefaction potential. *Journal of the Soil Mechanics and Foundations Division* 97(9), ASCE, 1249-1273.

Seed, H.B., Idriss, I.M., Makdisi, F. and Banerjee, N. (1975). Representation of irregular stress time histories by equivalent uniform stress series in liquefaction analyses. Report No. EERC 75-29, Earthquake Engineering Research Center, University of California, Berkeley, California.

Stokoe, K.H.,II, Nazarian, S., Rix, G.J., Sánchez-Salinero, I., Sheu, J.C. and Mok, Y.J. (1988). In situ seismic testing of hard-to-sample soils by surface wave method. *Earthquake Engineering and Soil Dynamics II - Recent Advances in Ground Motion Evaluation*, ASCE Geotechnical Special Publication No. 20, Von Thun, J.L., Ed., 264-278.

Stokoe, K.H.,II, Rix, G.J., Sánchez-Salinero, I., Andrus, R.D. and Mok, Y.J. (1989). Liquefaction of gravelly soils during the 1983 Borah Peak, Idaho earthquake. *Proc.* 9th World Conference on Earthquake Engineering III, 183-188.

Vucetic, M. and Dobry, R., (1988). Cyclic triaxial strain-controlled testing of liquefiable sands. *Advanced triaxial testing of soil and rock*, ASTM STP 977, Donaghe, R.T., Chaney, R.C. and Silver, M.L., Eds., ASTM, Philadelphia, 475-485.

Vucetic, M. and Dobry, R. (1991). Effect of soil plasticity on cyclic response. *Journal of Geotechnical Engineering* 117(1), 89-107.